Low temperature dynamics of nonlinear Luttinger liquids

2015 New J. Phys. 17 103003

(http://iopscience.iop.org/1367-2630/17/10/103003)

New Journal of Physics
The open access journal at the forefront of physics

Deutsche Physikalische Gesellschaft DPG
IOP Institute of Physics

Published in partnership with: Deutsche Physikalische Gesellschaft and the Institute of Physics

CrossMark

OPEN ACCESS

RECEIVED
15 June 2015

REVISED
7 August 2015

ACCEPTED FOR PUBLICATION
7 September 2015

PUBLISHED
30 September 2015

PAPER

Low temperature dynamics of nonlinear Luttinger liquids

C Karrasch[1,2], R G Pereira[3] and J Sirker[4,5,6]

[1] Department of Physics, University of California, Berkeley, CA 95720, USA
[2] Materials Sciences Division, Lawrence Berkeley National Laboratory, Berkeley, CA 94720, USA
[3] Instituto de Física de São Carlos, Universidade de São Paulo, C.P. 369, São Carlos, SP, 13560-970, Brazil
[4] Department of Physics and Research Center OPTIMAS, Technical University Kaiserslautern, D-67663 Kaiserslautern, Germany
[5] Department of Physics and Astronomy, University of Manitoba, Winnipeg, R3T 2N2, Canada
[6] Author to whom any correspondence should be addressed.

E-mail: sirker@physics.umanitoba.ca

Keywords: dynamical correlations, spin diffusion, Luttinger liquids, cold atomic gases

Abstract

We develop a general nonlinear Luttinger liquid theory to describe the dynamics of one-dimensional quantum critical systems at low temperatures. To demonstrate the predictive power of our theory we compare results for the autocorrelation $G(t)$ in the *XXZ* chain with numerical density-matrix renormalization group data and obtain excellent agreement. Our calculations provide, in particular, direct evidence that $G(t)$ shows a diffusion-like decay, $G(t) \sim 1/\sqrt{t}$, in sharp contrast to the exponential decay in time predicted by conventional Luttinger liquid theory.

1. Introduction

The dynamics of quantum critical systems at finite temperatures is an outstanding challenge in many-body physics [1]. Understanding the combined effects of thermal fluctuations and interactions is crucial for the interpretation of experiments that probe frequency-dependent responses and scattering cross sections. Addressing this problem has become even more pressing since fascinating new experiments in cold atomic gases [2–5] and condensed matter [6] have given us access to correlation functions directly in the time domain.

Much of the interest in real time evolution of many-body states has focused on one-dimensional (1D) models. In particular, the difference in the nonequilibrium dynamics of integrable versus nonintegrable systems is currently a hotly debated topic [7–11]. In parallel, studies of ground state dynamical correlations have recently forced us to revise our understanding of quasiparticles in critical 1D systems [12–20], culminating with the development of the nonlinear Luttinger liquid (NLL) theory [21]. This theory predicts that the long-time decay of correlation functions is dominated by excitations involving particles or holes near band edges, explaining the high-frequency oscillations observed numerically [22, 23] and confirmed by exact form factor approaches [24, 25].

The purpose of this work is to extend NLL theory to describe the low temperature, long time decay of correlation functions of 1D quantum fluids. Determining the precise effects of temperature is certainly relevant for experiments. Another motivation for this work is to provide analytic expressions to examine numerical results for time dependent correlation functions, accessible by finite-temperature versions [26–30] of time-dependent [31–35] density matrix renormalization group (tDMRG) methods [36, 37], and for the thermal broadening of edge singularities in the frequency domain [38]. To be specific, we will concentrate on the spin autocorrelation function $G(t)$ of the *XXZ* model at zero magnetic field, but our approach can easily be generalized to other correlations and 1D models. We stress that the time decay of correlation functions in the *XXZ* model at finite T is still an open problem despite the integrability of the model [39]. The main advantage of taking an integrable model as example is that many nonuniversal parameters in the field theory can be fixed [40, 41] allowing for a particularly rigorous numerical test. Our main results are: (i) $G(t)$ at intermediate times t is well described by a generalization of NLL theory that takes into account the effects of irrelevant operators on the dispersion of high-energy quasiparticles and on their coupling to low energy modes; (ii) at long times, $G(t)$

contains a non-oscillating, $\sim 1/\sqrt{t}$ decaying diffusion-like term, in sharp contrast to the exponential decay predicted by Luttinger liquid theory. Diffusive behavior in spins chains has been invoked to explain the spin-lattice relaxation rate [42] and muon-spin relaxation [43] measured in quasi-1D antiferromagnets and is attributed to inelastic umklapp scattering [40]. However, fingerprints of diffusion-like behavior have so far only been found indirectly in the current–current correlation function [28, 40, 44] and in the imaginary time dependence of the dynamical susceptibility [45]. Here we provide the first direct numerical evidence for a $1/\sqrt{t}$ long-time decay of the spin autocorrelation.

2. Model

Consider the 1D *XXZ* Hamiltonian

$$H = \sum_{j=1}^{L}\left(S_j^x S_{j+1}^x + S_j^y S_{j+1}^y + \Delta S_j^z S_{j+1}^z\right), \tag{1}$$

where S_j^a are spin-1/2 operators, Δ is the anisotropy parameter, and periodic boundary conditions are assumed. This model can be realized, for instance, in the Mott insulating phase of two-component Bose mixtures in 1D optical lattices [2, 46]. The spin autocorrelation function at temperature T is defined by

$$G(t) = \langle S_j^z(t) S_j^z(0)\rangle = \mathrm{Tr}\left\{S_j^z(t) S_j^z(0)\mathrm{e}^{-H/T}\right\}\Big/Z, \tag{2}$$

where $Z = \mathrm{Tr}\ \mathrm{e}^{-\mathrm{H}/T}$ is the partition function. Via the Jordan–Wigner transformation

$$S_j^z \rightarrow c_j^\dagger c_j - \frac{1}{2}, \qquad S_j^+ \rightarrow (-1)^j c_j^\dagger \exp\left(\mathrm{i}\pi \sum_{l<j} c_j^\dagger c_j\right), \tag{3}$$

the model (1) is equivalent to spinless fermions

$$H = \sum_{j=1}^{L}\left[-\frac{1}{2}\left(c_j^\dagger c_{j+1} + c_{j+1}^\dagger c_j\right) + \Delta\left(c_j^\dagger c_j - \frac{1}{2}\right)\left(c_{j+1}^\dagger c_{j+1} - \frac{1}{2}\right)\right], \tag{4}$$

where Δ plays the role of a nearest-neighbor density–density interaction. The spin inversion symmetry $S_j^z \rightarrow -S_j^z$ in the spin model (in the absence of a magnetic field) implies the particle–hole symmetry $c_j \rightarrow (-1)^j c_j^\dagger$ in the fermionic model. The latter sets the average density at half filling, $\langle c_j^\dagger c_j\rangle = 1/2$.

3. Noninteracting case

For $\Delta = 0$, the *XXZ* model reduces to a free fermion model. The autocorrelation factorizes into a product of free particle and hole Green's functions and is given exactly by [48]

$$G^{(0)}(t) = \langle c_j(t) c_j^\dagger(0)\rangle\langle c_j^\dagger(t) c_j(0)\rangle = \left(\int_{-\pi}^{\pi}\frac{\mathrm{d}k}{2\pi} f_k \mathrm{e}^{\mathrm{i}\epsilon_k t}\right)^2, \tag{5}$$

with dispersion $\epsilon_k = -\cos k$ and Fermi distribution $f_k = 1/(\mathrm{e}^{\epsilon_k/T} + 1)$ at half-filling.

Let us discuss an approximation that captures the asymptotic long-time decay of $G^{(0)}(t)$, and also of $\langle S_{j+r}^z(t) S_j^z(0)\rangle$ in the time-like regime $t \gg r$. First note that $G^{(0)}(t)$ oscillates at arbitrary temperatures due to saddle points of the integrand where $\mathrm{d}\epsilon_k/\mathrm{d}k = 0$, which occur at $k = 0$ and $k = \pi$. For $T \ll 1$, we can employ a mode expansion of the fermion field which keeps only states within sub-bands near the smeared Fermi surface and near the saddle points, in the form

$$c_{j=x} \sim \psi_\mathrm{R}(x)\mathrm{e}^{\mathrm{i}\pi x/2} + \psi_L(x)\mathrm{e}^{-\mathrm{i}\pi x/2} + \bar{d}^\dagger(x) + \mathrm{e}^{\mathrm{i}\pi x} d(x). \tag{6}$$

Here $\psi_{\mathrm{R,L}}$ are the low-energy right- and left-moving components, while $\bar{d}$ and d are high-energy modes: $\bar{d}^\dagger$ creates a hole at the bottom of the band ($k = 0$), and d annihilates a particle at the top of the band ($k = \pi$).

The mode expansion reduces the problem to the calculation of free propagators for $\psi_{\mathrm{R,L}}$ and d, $\bar{d}$. The low energy modes have linear dispersion, thus their propagator at $T \ll 1$ is given by the standard conformal field theory result $\langle\psi_{\mathrm{R,L}}(x, t)\psi_{\mathrm{R,L}}^\dagger(x, 0)\rangle \sim \pi T/\sinh(\pi T t)$. On the other hand, the high-energy modes do not feel the temperature, up to an exponentially small correction in the Fermi distribution. Since the dispersion is parabolic near the band edges, $\epsilon_k \approx 1 - k^2/2$, the propagator of d, $\bar{d}$ decays slowly, $\langle d(x, t) d^\dagger(x, 0)\rangle \sim \mathrm{e}^{-\mathrm{i}t}/\sqrt{t}$. Substituting the contributions from low and high energy modes into equation (5), we obtain the asymptotic decay of $G^{(0)}(t)$:

$$G^{(0)}(t) \approx \frac{\mathrm{i}e^{-\mathrm{i}2t}}{2\pi t} + \frac{\sqrt{2}\,T e^{-\mathrm{i}(t+\pi/4)}}{\sqrt{\pi t}\,\sinh(\pi T t)} - \frac{T^2}{\sinh^2(\pi T t)}. \tag{7}$$

The first term stems from the contribution in which both particle and hole are high-energy modes. The second term is due to a high-energy particle (hole) plus a low-energy hole (particle) at either one of the Fermi points. The latter decays exponentially for $t \gg 1/T$. The third contribution is due only to the low-energy modes $\psi_{\mathrm{R,L}}$, and decays more rapidly than the oscillating terms. Therefore, $G^{(0)}(t)$ for $t \gg 1/T$ is dominated by the term oscillating with frequency $\omega = 2$ and decaying as $1/t$.

4. Interacting case: NLL theory

We focus on the regime $0 < \Delta < 1$ corresponding to a critical phase of fermions with repulsive interactions. The factorization of $G(t)$ as in equation (5) is then *a priori* lost. However, we can investigate the long-time decay of $G(t)$ using the framework of NLL theory [21]. The idea is to keep the mode expansion, equation (6), with both low- and high-energy modes, which are now identified as quasiparticles in a renormalized band. The ground state is a vacuum of d and $\bar{d}$, and the spin operator $S_j^z \sim c_j^\dagger c_j$ creates at most one d particle and/or one $\bar{d}$ hole. At low temperatures, we neglect an exponentially small thermal population of the band edge modes. The d, $\bar{d}$ quasiparticles can then be treated as mobile 'impurities' distinguishable from the low-energy modes. We note, however, that an exponentially small relaxation rate associated with thermally activated holes near the bottom of the band has been discussed in the context of conductance in quantum wires [18]. Such processes would only affect the real-time dependence of correlation functions after exponentially long times and will be neglected here.

At $T = 0$ the dynamics is described by an effective field theory with Hamiltonian density [22]

$$\begin{aligned}\mathcal{H} = {} & d^\dagger\left(\varepsilon + \frac{\partial_x^2}{2\,m}\right)d + \bar{d}^\dagger\left(\varepsilon + \frac{\partial_x^2}{2\,m}\right)\bar{d} + V d^\dagger d\,\bar{d}^\dagger\bar{d} \\ & + \frac{v}{2}\left[\left(\partial_x\theta\right)^2 + \left(\partial_x\phi\right)^2\right] + \frac{v\alpha}{\sqrt{\pi K}}\partial_x\phi\left(d^\dagger d - \bar{d}^\dagger\bar{d}\right).\end{aligned} \tag{8}$$

Here ε is the energy and m the absolute value of the effective mass of the band edge modes, V is the impurity-impurity interaction, $\phi(x)$ and $\theta(x)$ are dual fields representing the bosonized low-energy modes [47] and obey $[\phi(x), \partial_{x'}\theta(x')] = \mathrm{i}\delta(x - x')$. v is the spin velocity, K the Luttinger parameter, and α the dimensionless coupling constant of the impurity-boson interaction. For the integrable XXZ model one finds $v = \varepsilon = \frac{1}{m} = \frac{\pi\sqrt{1-\Delta^2}}{2\arccos\Delta}$, $K = 1 - \frac{\alpha}{2\pi} = \frac{\pi/2}{\pi - \arccos\Delta}$, while $V \approx -4\Delta$ for $\Delta \ll 1$.

Equation (8) must be regarded as a fixed point Hamiltonian which includes all *marginal* interactions allowed by symmetry. This model can be solved exactly by performing a unitary transformation that decouples the impurities from the bosonic modes, but attaches 'string' operators to the d, $\bar{d}$ fields [14]:

$$d(x) \to d(x)e^{-\mathrm{i}\alpha\theta(x)/\sqrt{\pi K}}, \tag{9}$$

$$\bar{d}(x) \to \bar{d}(x)e^{\mathrm{i}\alpha\theta(x)/\sqrt{\pi K}}. \tag{10}$$

The calculation of the free correlators in the effective field theory after the unitary transformation allows one to predict the long-time decay of $G(t)$ at $T = 0$, up to non-universal amplitudes [22].

We now extend the NLL theory to $0 < T \ll \varepsilon$, where ε is the renormalized bandwidth. We obtain the leading T dependence by analyzing the effects of *irrelevant* interactions. The leading corrections to the oscillating terms in $G(t)$ allowed by symmetry (see appendix A) stem from the irrelevant dimension-three operators

$$\begin{aligned}\delta\mathcal{H} = {} & g\left[\left(\partial_x\theta\right)^2 + \left(\partial_x\phi\right)^2\right]\left(d^\dagger d + \bar{d}^\dagger\bar{d}\right) \\ & + g'\left[\left(\partial_x\theta\right)^2 - \left(\partial_x\phi\right)^2\right]\left(d^\dagger d + \bar{d}^\dagger\bar{d}\right) - \mu_+\partial_x^2\theta\left(d^\dagger d - \bar{d}^\dagger\bar{d}\right) \\ & + \mu_-\partial_x\theta\left(-\mathrm{i}d^\dagger\partial_x d + \mathrm{i}\bar{d}^\dagger\partial_x\bar{d} + \mathrm{h.c.}\right).\end{aligned} \tag{11}$$

Substituting the mode expansion into Hamiltonian (1) and bosonizing the low-energy modes, we find for $\Delta \ll 1 : g \approx -\Delta$, $\mu_- \approx -\Delta/\sqrt{\pi}$, while g' and μ_+ are zero to first order in Δ. The g' interaction can be identified with a three-body scattering process [16, 22] and gives rise to a nonzero impurity decay rate for $T > 0$ [49, 50]. By imposing nontrivial conservation laws in the XXZ model we can show that $g' = 0$ exactly [51] (see appendix A for details), as expected from the lack of three-body scattering in integrable models.

In contrast with the noninteracting result in equation (7), in the interacting case the irrelevant operators can modify both frequencies and exponents of the high-energy terms of $G(t)$. To investigate this effect, we calculate the impurity self-energy Σ and effective impurity-boson interaction $\tilde{\alpha}$ by perturbation theory in the irrelevant operators (see appendix B for details). The leading T dependence is determined by loop diagrams which contain only one irrelevant coupling constant but arbitrary factors of the bare α. In the calculation of loop diagrams, it is convenient to treat the quadratic term in the impurity dispersion (which is also a dimension-three operator) as a perturbation, expanding the internal impurity propagators in powers of $1/m$. We find

$$\Sigma(T) \approx c_\Sigma T^2/v^2, \tag{12}$$

$$\tilde{\alpha}(T) \approx \alpha\left(1 + c_\alpha T/v^2\right). \tag{13}$$

The prefactors c_Σ and c_α are linear functions of $g,\ \mu_+,\ \mu_-$. Bearing in mind that $g,\ \mu_- \sim \mathcal{O}(\Delta),\ \mu_+ \sim \mathcal{O}(\Delta^2)$ for $\Delta \ll 1$, we obtain the weak coupling approximation

$$c_\Sigma \approx \frac{\pi g}{3} + \frac{\alpha^2}{12Km}, \tag{14}$$

$$c_\alpha \approx -2g + \frac{\alpha^2}{2\pi Km}. \tag{15}$$

Omitted terms are $\mathcal{O}(\Delta^3)$ or higher. To first order in Δ, the self-energy and vertex correction are both governed by $g \approx -\Delta$. For $0 < \Delta \ll 1$, equation (13) thus implies that the effective impurity energy $\tilde{\varepsilon}(T) = \varepsilon + \Sigma(T)$ decreases $\sim T^2$, whereas the effective coupling $\tilde{\alpha}$ increases linearly with T. Phenomenologically, we find $g = \frac{\pi v^2}{2K}\frac{\partial^2\varepsilon}{\partial h^2}\,|_{h=0}$ relating the coupling constant g in equation (11) to a change in the impurity energy when applying a magnetic field h. This allows one to obtain $g\,(\Delta)$ exactly using the Bethe ansatz and Wiener-Hopf techniques. Unfortunately, the corrections of higher order in α in equation (13) quickly become of the same order as the $\mathcal{O}(g)$ term making it impossible to fix $c_\Sigma,\ c_\alpha$ beyond the lowest order in Δ. Importantly however, the T dependence of $\tilde{\varepsilon}$ and $\tilde{\alpha}$ holds for arbitrary $0 < \Delta < 1$, as long as the temperature is small enough.

The integrability of the *XXZ* chain suggests that one might be able to relate the oscillation frequency $\tilde{\varepsilon}(T)$ with the so-called dressed energy in the thermodynamic Bethe ansatz. We will discuss this point in appendix C.

The renormalization of the impurity-impurity interaction appears at order g^2. The basic process involves a two-boson loop connecting two impurity lines. The correction depends on the momentum and frequency exchange between the impurities: $\tilde{V}(q,\ \omega,\ T) \approx V + \frac{2\pi g^2\, T^2\omega}{3v^4 q}$, where we simplified the result in the physically relevant regime $\omega \ll vq$ for impurities with parabolic dispersion.

We can now describe the decay of $G(t)$ using the methods of NLL theory with renormalized parameters at $T > 0$. First, consider the contribution from the excitation with a single impurity, equivalent to the second term in equation (7). The unitary transformation introduces a 'string' operator whose scaling dimension depends on temperature through $\tilde{\alpha}(T)$. The result is

$$G_1(t) \approx \frac{A(T)}{\sqrt{t}}\left[\frac{\pi T}{\sinh(\pi T t)}\right]^{\tilde{\eta}(T)} \mathrm{e}^{-i\left[\tilde{\varepsilon}(T)t + \tilde{\varphi}(T)\right]}, \tag{16}$$

where $\tilde{\eta}(T) = \frac{K}{2} + \frac{1}{2K}\left[1 - \frac{\tilde{\alpha}(T)}{2\pi}\right]^2$, $\tilde{\varphi}(T) = \frac{\pi}{2}\left[\tilde{\eta}(T) - \frac{1}{2}\right]$, and $A(T)$ is the unknown prefactor. Note that $\tilde{\alpha}(T) > \alpha$ for $0 < \Delta \ll 1$ implies that $\tilde{\eta}(T)$ decreases with temperature, slightly slowing down the decay of $G_1(t)$.

The two-impurity contribution to $G\,(t)$, analogous to the first term in equation (7), is strongly modified by the V interaction. At $T = 0$, the $1/t$ decay for $\Delta = 0$ changes to $1/t^2$ for $\Delta > 0$ and $t \gg 1/V^2$ [22]. This asymptotic behavior is associated with two impurities scattering in a ladder series with small energy and momentum transfer, $\omega \sim q^2/m \ll \varepsilon$. Neglecting the renormalization of V for $\omega \ll vq$, we obtain the two-impurity contribution

$$G_2(t) \approx \frac{B(T)}{t^2}\, \mathrm{e}^{-i2\tilde{\varepsilon}(T)t}, \tag{17}$$

where $B(T)$ is the unknown prefactor.

The results for the high-energy terms in equations (16) and (17) hold for the integrable *XXZ* model, but can be extended to generic models by considering the effects of nonzero three-body scattering amplitude g'. The main effect associated with integrability breaking is that the high-energy excitations acquire a finite decay rate at $0 < T \ll \varepsilon$. In the particle–hole symmetric case, the decay rate of both d and $\bar{d}$ modes is equivalent to the hole relaxation rate derived in [50], $1/\tau \sim (g')^2(T/\varepsilon)^2$. In real time, the impurity relaxation introduces an additional exponential decay $\sim \mathrm{e}^{-t/\tau}$ for $t \gg \tau$. At low temperatures the effect is negligible for the one-impurity contribution in equation (16) (which already decays exponentially within a time scale that scales linearly with T) but should become important to analyze the two-impurity contribution in equation (17) for times $t \gtrsim \tau$.

5. Diffusive decay

At temperatures $T \ll 1$, conventional Luttinger liquid theory predicts that the non-oscillating terms in $G(t)$, associated only with the low-energy modes $\psi_{\mathrm{R,L}}$, decay exponentially

$$G_{\mathrm{LL}}(t) \approx A' \left[\frac{\pi T}{\sinh(\pi T t)} \right]^2 + B' \left[\frac{\pi T}{\sinh(\pi T t)} \right]^{2K}, \tag{18}$$

with known amplitudes A', B' [52]. However, we must also consider how irrelevant operators affect the low-energy contributions. In [40] it was shown that the formally irrelevant umklapp scattering

$$\delta\mathcal{H}_U = \lambda \cos\left(4\sqrt{\pi K}\phi\right) \tag{19}$$

qualitatively changes the long-time decay of the low-energy, long-wavelength contribution to $G(t)$. There appears a new time scale set by the decay rate

$$\gamma = C(K) \left(\frac{2\pi}{v} \right)^{4K-2} \lambda^2 \, T^{8K-3}, \tag{20}$$

where $C(K)$ is a prefactor given by [40]

$$C(K) = \frac{2\pi K \sin(2\pi K)}{\sqrt{\pi}\, 2^{2K+1}} \Gamma\left(\frac{1}{2} - K \right) \Gamma(K) B(K, 1 - 2K) \cot(\pi K), \tag{21}$$

where $\Gamma(x)$ denotes the gamma function and $B(x, y) = \Gamma(x)\Gamma(y)/\Gamma(x + y)$ is the beta function. For the *XXZ* model, γ can be calculated exactly using the result for the umklapp coupling constant [52]

$$\lambda = \frac{K\Gamma(K)\sin(\pi/K)}{\pi\Gamma(2 - K)} \left[\frac{\Gamma\left(1 + \frac{1}{2K - 2}\right)}{2\sqrt{\pi}\,\Gamma\left(1 + \frac{K}{2K - 2}\right)} \right]^{2K-2}. \tag{22}$$

In [40] it was shown that including a nonzero decay rate in the boson propagator leads to the long-wavelength term in $G(t)$ given by

$$G_{q=0}(t) \approx \frac{K}{2\pi v^2} \int_{-\infty}^{\infty} \frac{\mathrm{d}\omega}{4\pi} \frac{\mathrm{e}^{-\mathrm{i}\omega t}}{1 - \mathrm{e}^{-\beta\omega}} \left[\left(\omega^2 + 2\mathrm{i}\gamma\omega\right)^{1/2} + \left(\omega^2 - 2\mathrm{i}\gamma\omega\right)^{1/2} \right]. \tag{23}$$

For $\gamma = 0$ the calculation simplifies as the integrand in equation (23) only has poles in the complex plane; in this case one recovers the standard result in equation (18). For $\gamma > 0$, one obtains an additional contribution from the branch cut of the integrand. The result simplifies in the regime of very long times $t \gg 1/\gamma \gg 1/T$; in addition to equation (18) we find the extra term[7]

$$G_{\mathrm{diff}}(t) = \frac{\Gamma}{\sqrt{t}}, \quad \Gamma = \frac{KT}{\pi v^2} \sqrt{\frac{\gamma}{2\pi}}. \tag{24}$$

More generally, in the regime $|r|/v \ll 1/\gamma \ll t$ one obtains $\langle S^z_{j+r}(t) S^z_j(0) \rangle \sim \Gamma \mathrm{e}^{-\gamma r^2/2v^2 t} / \sqrt{t}$. This is exactly the behavior predicted by the phenomenological diffusion theory, based on a random walk of the magnetization through the 1D lattice [53–55]. Note, however, that the diffusion-like decay is limited to a certain space-time and temperature domain. The assumptions of independent modes in the phenomenological theory of spin diffusion do not hold in a 1D quantum fluid and the full space and time dependence of correlations is not captured.

The debate about the existence of spin diffusion in integrable spin chains has a long, controversial history [26, 40, 42, 48, 56–66]. At first sight, our claim that the long time decay of $G(t) \sim T^{4K-1/2}/\sqrt{t}$ is diffusion-like may sound contradictory because it has been proven recently that the critical *XXZ* chain exhibits a nonzero Drude weight at arbitrarily high temperatures [67–69]. The latter implies *ballistic* spin transport [70, 71]. However, it is important to note that the Drude weight is related to the long-time decay of the total spin *current*, whereas the diffusion-like decay arises in the correlation for the local spin *density*. Clearly, the conventional phenomenology cannot account for all the dynamical properties of 1D quantum fluids at low T. A striking indication of this is in fact that for integrable systems ballistic transport may coexist with a diffusion-like decay in the spin density correlation. Note that by breaking integrability, e.g. by a next-nearest neighbor interaction, the dc conductivity will become finite while the $1/\sqrt{t}$ decay of the spin autocorrelation is generic. To establish our claim beyond the approximations of the field theory approach, in the following we shall exhibit direct numerical confirmation for the diffusion-like decay in the *XXZ* chain.

[7] Note that this corrects the result in [40] where a factor 2π is missing.

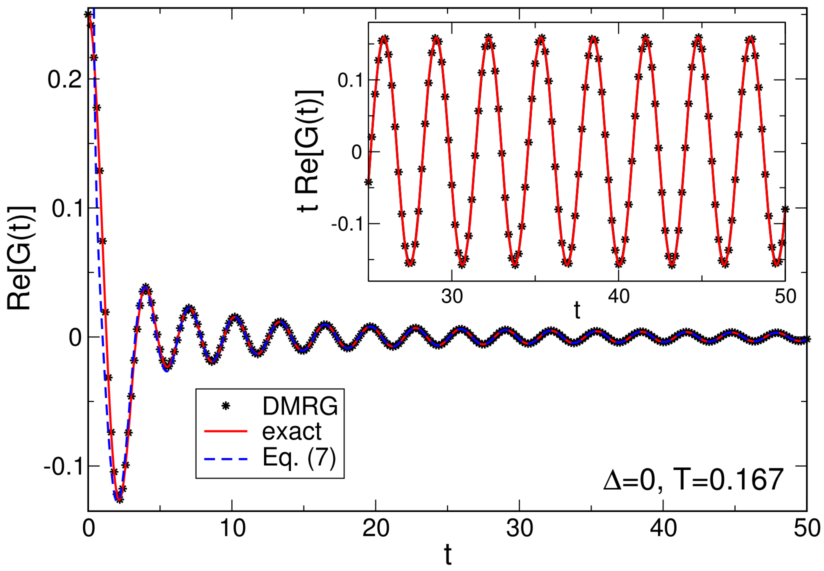

Figure 1. Real part of the spin autocorrelation $G(t)$ in the noninteracting case $\Delta = 0$ for temperature $T = 0.167$. The DMRG data (symbols) are in perfect agreement with the exact result (red solid line). The blue dashed line shows that the approximation, equation (7), is excellent except for very short times. The inset shows that at long times $tG(t)$ oscillates with constant amplitude, confirming the dominant $1/t$ decay for $\Delta = 0$.

6. Numerical results

We now turn to a comparison of our theory with tDMRG results for finite system size. Rather than exploring the full space–time dependence of the spin–spin correlation function, here we focus on the autocorrelation since our main goal is to analyze the asymptotic long-time behavior where conventional Luttinger liquid theory breaks down. (More generally, for correlations at finite distance r the high-energy contributions associated with band edge modes are observed inside the light cone for times $t \gg r/v$.) Non-zero temperatures are incorporated via a purification of the density matrix. By using the disentangler introduced in [28] and exploiting time translation invariance $\langle S_j^z(t) S_j^z(0)\rangle = \langle S_j^z(t/2) S_j^z(-t/2)\rangle$ [30] we can substantially extend the accessible time scale. Details of the algorithm are described in [29, 37]. The two parameters which determine the accuracy of the DMRG results are the system size and the discarded weight. We carry out all our calculations using $L = 200$ sites; this is sufficient to reproduce the exact thermodynamic-limit result at $\Delta = 0$ up to times $t = 50$ (see figure 1). At finite Δ, we have examplarily performed calculations using $L = 300$ to ensure that for the temperatures and time scales considered our results are effectively in the thermodynamic limit. For each set of parameters $\{\Delta, T\}$, we carry out the DMRG calculations using four discarded weights which each differ by a factor of 10. We stop the calculation once the bond dimension reaches a value of 2000. This allows us to estimate the truncation error, which in all cases is smaller than the symbol size.

Apart from demonstrating the accuracy of the numerical data, figure 1 also confirms that for $\Delta = 0$ and $T > 0$ the long-time behavior of $G(t)$ is dominated by the two-impurity term oscillating with frequency $\omega = 2$ and decaying as $1/t$.

We now turn to the interacting case. We find a striking difference between the weakly interacting case, figure 2, and the strongly interacting case, figure 3. While the data for $\Delta = 0.8$ can be very well fitted by a sum of the single impurity contribution (16) and the diffusive part (24), it is necessary to also include the two-impurity contribution (17) for $\Delta = 0.3$. In the latter case, we also allow for an additional decay rate ρ by multiplying equation (17) by $e^{-\rho t}$. The fits yield very small decay rates which seem to be of order $\sim e^{-1/T}$ and could possibly be related to thermal excitations at the band edges which we have neglected in our analysis (see appendix D for details).

The values of the decay rate γ due to Umklapp scattering predicted by our theory are so small that we are not able to access the regime $t \gg 1/\gamma$ in which the simple expression (24) has been derived. (For instance, we have $1/\gamma \approx 55$ for $\Delta = 0.8$ and $T = 0.25$.) A numerical solution of equation (23), however, shows that $\sqrt{t}\,G(t)$ already reaches the plateau predicted by equation (24) at much earlier times, times which we are able to investigate by tDMRG. In practice, we search for a diffusive-like term in the form of a nonzero asymptotic value of Re $[\sqrt{t}\,G(t)]$ at long times. At $T = 0.25$ we find for both Δ values clear evidence for a diffusion-like decay with diffusion constants $\Gamma_{\rm fit}$ close to the predicted values, $\Gamma_{\rm th}$, see equation (24). In addition, we find numerically that

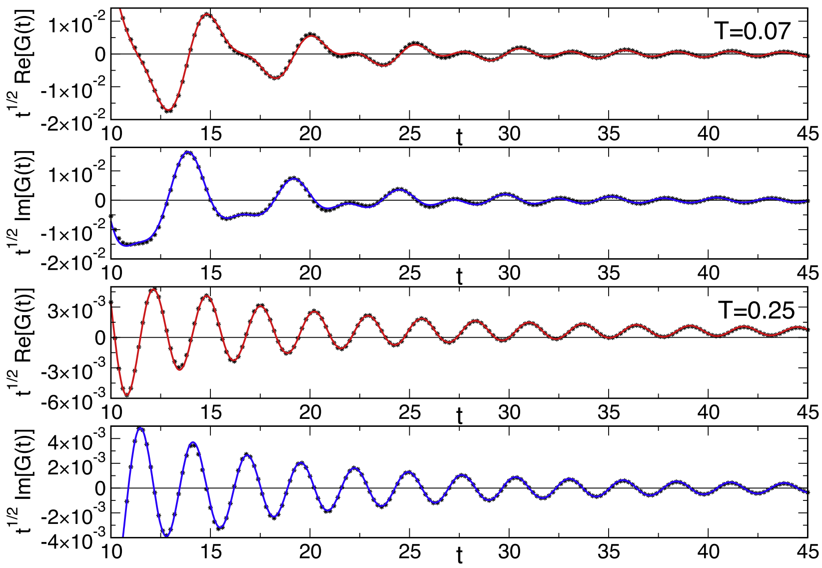

Figure 2. $\sqrt{t}\,G(t)$ at $\Delta = 0.3$: tDMRG data (symbols) and fits (lines) for $t \geqslant 10$. Here $\lim_{t\to\infty}\sqrt{t}\,G(t) = \Gamma$ with $\Gamma_{\rm fit}(T = 0.07) \approx 0$ [$\Gamma_{\rm th}(T = 0.07) = 2.1 \times 10^{-5}$] and $\Gamma_{\rm fit}(T = 0.25) \approx 6.3 \times 10^{-4}$ [$\Gamma_{\rm th}(T = 0.25) = 7.9 \times 10^{-4}$].

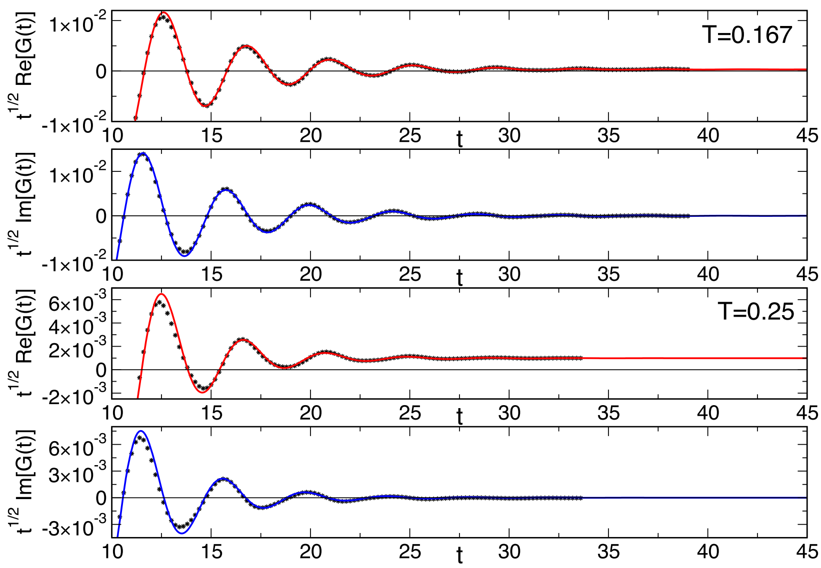

Figure 3. Same as figure 2 for $\Delta = 0.8$ with $\Gamma_{\rm fit}(T = 0.167) \approx 3.3 \times 10^{-4}$ [$\Gamma_{\rm th}(T = 0.167) = 5.6 \times 10^{-4}$] and $\Gamma_{\rm fit}(T = 0.25) \approx 9.9 \times 10^{-4}$ [$\Gamma_{\rm th}(T = 0.25) = 1.3 \times 10^{-3}$].

in agreement with our theory the $1/\sqrt{t}$ contribution seems to vanish for magnetic fields $h \gg T$ where the Umklapp term (19) is oscillating and should be dropped [40]. This is exemplarily shown in figure 4, demonstrating that $G(t)$ decays faster than $1/\sqrt{t}$ in this case.

The oscillation frequency $\tilde{\varepsilon}(T)$ and exponent $\tilde{\eta}(T)$, obtained from fits of tDMRG data at $\Delta = 0.3$ and zero magnetic field, are shown in figure 5. The data confirm that $\tilde{\varepsilon} \sim -T^2$ and $\tilde{\eta} \sim -T$ while the prefactors, even for $\Delta = 0.3$, already seem to deviate significantly from the lowest order result in equation (15).

7. Conclusion

Finite temperatures and quantum fluctuations lead to large non-perturbative effects on dynamical correlations in NLL's. The exponents of oscillating contributions are renormalized by temperature while umklapp scattering leads to a diffusion-like term dominating the long-time asymptotics. These predictions are in excellent agreement with tDMRG results which provide, in particular, the first direct evidence for a diffusion-like decay of

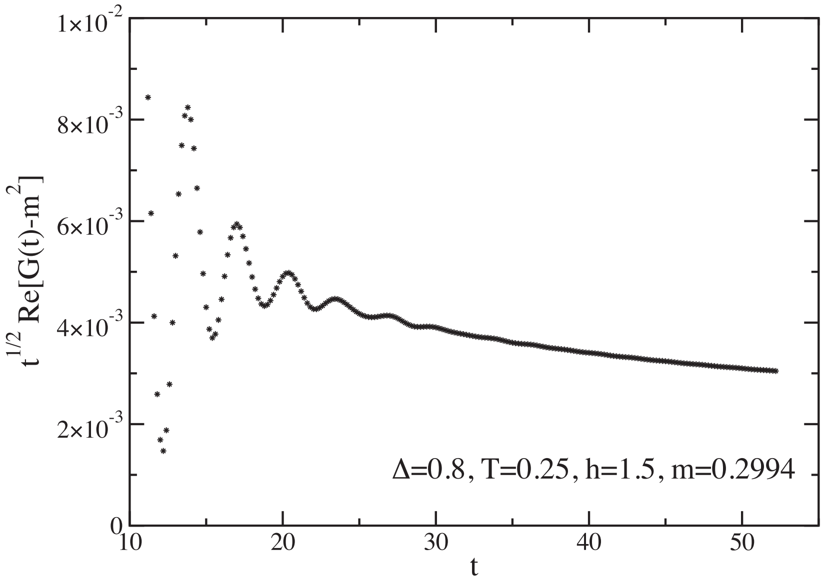

Figure 4. Real part of $G(t) - m^2$ for finite magnetization m. The connected part of $\mathrm{Re}[G(t)]$ decays faster than $1/\sqrt{t}$ for $h \gg T$.

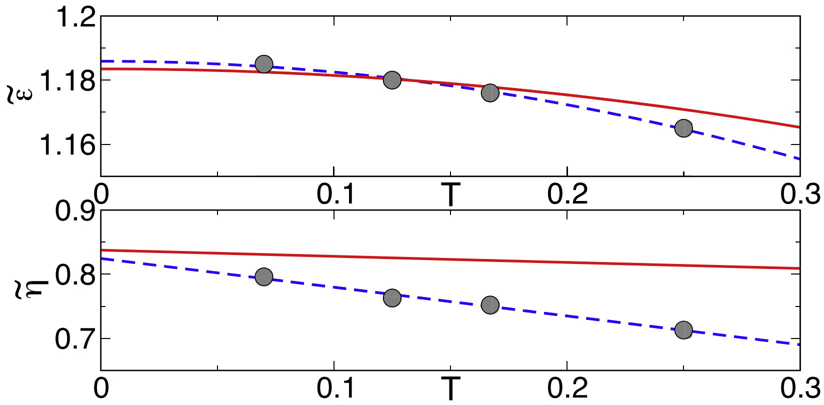

Figure 5. $\tilde{\varepsilon}(T)$ and $\tilde{\eta}(T)$ for $\Delta = 0.3$ from fits of tDMRG data (symbols). Dashed lines: quadratic and linear least square fits, respectively; solid lines: $\mathcal{O}(\Delta)$ theoretical result, equation (13).

spin correlations in the *XXZ* model and show striking changes in the one- and two-impurity contributions as a function of temperature and interaction strength. We expect that the coexistence of a diffusion-like decay of the autocorrelation with a ballistic propagation of the spin current can soon be tested experimentally in cold atomic gases [3, 5]. The theory presented here is not restricted to integrable models and can easily be extended to systems such as Bose or Fermi gases, or to study the propagation of impurities through 1D quantum fluids at finite temperatures. The calculation of decay rates for the Bose gas at finite T, in particular, is now within reach which should help to shed light on the experimentally observed evolution from a prethermalized to a fully equilibrated state following a quantum quench [72].

Acknowledgments

We thank FHL Essler, LI Glazman, A Klümper and M Panfil for helpful discussions. JS acknowledges support by the Collaborative Research Centre SFB/TR49, the Graduate School of Excellence MAINZ (DFG, Germany), as well as NSERC (Canada). RGP acknowledges support by CNPq (Brazil). CK acknowledges support by Nanostructured Thermoelectrics program of LBNL.

Appendix A. Irrelevant impurity-boson interactions

In this section we discuss the general kinematic structure of the low-energy effective theory by considering discrete symmetries and then show that integrability of the *XXZ* model further constrains the coupling constants of irrelevant operators.

Particle–hole (C) and parity (P) transformations act on the bosonic fields and impurity fields as follows [52]:

$$C:\begin{cases}\theta & \to & -\theta\\ \phi & \to & -\phi\\ d & \to & \bar{d}\\ \bar{d} & \to & d\end{cases},\quad P:\begin{cases}x & \to & -x\\ \theta & \to & \theta\\ \phi & \to & -\phi\\ d & \to & d\\ \bar{d} & \to & \bar{d}\end{cases}. \tag{A.1}$$

The Hamiltonian can only contain operators that are invariant under C and P. Let us denote by $H_a^{(n)} = \int \mathrm{d}x\ \mathcal{H}_a^{(n)}(x),\ a = 1, 2, ...$, a particular term in the Hamiltonian such that $\mathcal{H}_a^{(n)}$ is an operator with scaling dimension n. Up to dimension four, we have a list of 14 operators allowed by symmetry:

$$\begin{aligned}
\mathcal{H}_1^{(2)} &= \frac{v}{2}\left[\left(\partial_x\theta\right)^2 + \left(\partial_x\phi\right)^2\right],\\
\mathcal{H}_2^{(1)} &= \varepsilon\left(d^\dagger d + \bar{d}^\dagger\bar{d}\right),\\
\mathcal{H}_3^{(3)} &= -\frac{1}{2\,m}\left(\partial_x d^\dagger\partial_x d + \partial_x\bar{d}^\dagger\partial_x\bar{d}\right),\\
\mathcal{H}_4^{(2)} &= \frac{v\alpha}{\sqrt{\pi K}}\partial_x\phi\left(d^\dagger d - \bar{d}^\dagger\bar{d}\right),\\
\mathcal{H}_5^{(2)} &= -Vd^\dagger d\bar{d}^\dagger\bar{d},\\
\mathcal{H}_6^{(3)} &= g\left[\left(\partial_x\theta\right)^2 + \left(\partial_x\phi\right)^2\right]\left(d^\dagger d + \bar{d}^\dagger\bar{d}\right),\\
\mathcal{H}_7^{(3)} &= g'\left[\left(\partial_x\theta\right)^2 - \left(\partial_x\phi\right)^2\right]\left(d^\dagger d + \bar{d}^\dagger\bar{d}\right),
\end{aligned}$$

$$\begin{aligned}
\mathcal{H}_8^{(3)} &= \mu_+\partial_x\theta\ \partial_x\left(d^\dagger d - \bar{d}^\dagger\bar{d}\right),\\
\mathcal{H}_9^{(3)} &= -\mathrm{i}\mu_-\partial_x\theta\left(d^\dagger\partial_x d - \partial_x d^\dagger d - \bar{d}^\dagger\partial_x\bar{d} + \partial_x\bar{d}^\dagger\bar{d}\right),\\
\mathcal{H}_{10}^{(4)} &= \vartheta_+\left(d^\dagger\partial_x d\partial_x d^\dagger d + \bar{d}^\dagger\partial_x\bar{d}\partial_x\bar{d}^\dagger\bar{d}\right),\\
\mathcal{H}_{11}^{(4)} &= \vartheta_-\left(d^\dagger\partial_x d - \partial_x d^\dagger d\right)\left(\bar{d}^\dagger\partial_x\bar{d} - \partial_x\bar{d}^\dagger\bar{d}\right),\\
\mathcal{H}_{12}^{(4)} &= \mathrm{i}\kappa_1\partial_x^2\phi\left(d^\dagger\partial_x d - \partial_x d^\dagger d - \bar{d}^\dagger\partial_x\bar{d} + \partial_x\bar{d}^\dagger\bar{d}\right),\\
\mathcal{H}_{13}^{(4)} &= \mathrm{i}\kappa_2\partial_x\phi\partial_x\theta\left(d^\dagger\partial_x d - \partial_x d^\dagger d + \bar{d}^\dagger\partial_x\bar{d} - \partial_x\bar{d}^\dagger\bar{d}\right),\\
\mathcal{H}_{14}^{(4)} &= \kappa_3\partial_x\phi\left(\partial_x d^\dagger\partial_x d - \partial_x\bar{d}^\dagger\partial_x\bar{d}\right).
\end{aligned} \tag{A.2}$$

All the operators in equation (A.2) conserve the total number of particles and holes in the high-energy subbands. In the above list we have omitted operators which couple the impurity modes to umklapp type operators. The lowest dimension operator in this family is $(d^\dagger d + \bar{d}^\dagger\bar{d})\cos\,(4\sqrt{\pi K}\,\phi)$, whose scaling dimension varies continuously from 5 at $\Delta = 0$ to 3 at $\Delta = 1$. The set of constraints on the coupling constants that we shall derive in the following is not affected by this family of operators.

The integrability of the *XXZ* model affects the effective impurity model by constraining the coupling constants of irrelevant interactions. Following [15], we shall examine the consequences of integrability by imposing the existence of nontrivial conservation laws. For the *XXZ* model, it is fortunate that the first nontrivial conserved quantity can be identified with the energy current operator J_{E}, which is defined from the continuity equation for the Hamiltonian density [51]. In the continuum limit, the energy current density is given by

$$\partial_x j(x) = \mathrm{i}[\mathcal{H}(x), H], \tag{A.3}$$

where $H = \int \mathrm{d}x\ \mathcal{H}(x) = \sum_a \int \mathrm{d}x\ \mathcal{H}_a$ is the total Hamiltonian. The energy current operator is $J_{\mathrm{E}} = \int \mathrm{d}x\ j(x)$. Let us denote by $j_{a,b}$, with $a < b$, the contribution to the energy current density obtained by taking the commutator of terms $\mathcal{H}_a$ and $\mathcal{H}_b$ in the Hamiltonian as follows:

$$\partial_x j_{a,b}^{(n+m-2)} = \mathrm{i}\int dy \left\{ \left[\mathcal{H}_a^{(n)}(x), \mathcal{H}_b^{(m)}(y)\right] + \left[\mathcal{H}_b^{(m)}(x), \mathcal{H}_a^{(n)}(y)\right] - \delta_{ab}\left[\mathcal{H}_a^{(n)}(x), \mathcal{H}_a^{(n)}(y)\right]\right\}. \tag{A.4}$$

The notation implies that when we take the commutator of a dimension-n operator with another dimension-m operator, the corresponding contribution to J_{E} (when nonvanishing) has dimension $n + m - 2$.

To check that $J_{\mathrm{E}} = \sum_{a<b} J_{a,b}$ is conserved, we need to take the commutator with all the terms in H again:

$$\left[J_{a,b}^{(n+m-2)}, H_c^{(l)}\right] = \int \mathrm{d}x\ \mathcal{O}_{a,b,c}^{(n+m+l-1)}(x). \tag{A.5}$$

We organize the expansion by operator dimension. In order to find nontrivial relations between the coupling constants in equation (A.2), it suffices to compute $[J_{\mathrm{E}}, H]$ to the level of dimension-four operators. For this we need to consider up to dimension-three operators in J_{E}. We find the following list of operators

$$\begin{aligned}
j_{1,1}^{(2)} &= -\,v^2\partial_x\theta\partial_x\phi,\\
j_{2,3}^{(2)} &= \frac{\mathrm{i}\varepsilon}{m}\left(d^\dagger\partial_x d + \bar{d}^\dagger\partial_x\bar{d}\right),\\
j_{1,4}^{(2)} &= -\,\frac{\alpha v^2}{\sqrt{\pi K}}\partial_x\theta\left(d^\dagger d - \bar{d}^\dagger\bar{d}\right),\\
j_{3,4}^{(3)} &= \frac{\mathrm{i}\alpha v}{2\,m\sqrt{\pi K}}\partial_x\phi\left(d^\dagger\partial_x d - \partial_x d^\dagger d - \bar{d}^\dagger\partial_x\bar{d} + \partial_x\bar{d}^\dagger\bar{d}\right),\\
j_{3,5}^{(3)} &= -\,\frac{\mathrm{i}V}{2\,m}\left[\bar{d}^\dagger\bar{d}\left(d^\dagger\partial_x d - \partial_x d^\dagger d\right) + d^\dagger d\left(\bar{d}^\dagger\partial_x\bar{d} - \partial_x\bar{d}^\dagger\bar{d}\right)\right],\\
j_{1,6}^{(3)} &= -\,4gv\partial_x\theta\partial_x\phi\left(d^\dagger d + \bar{d}^\dagger\bar{d}\right),\\
j_{1,8}^{(3)} &= -\,\mu_+ v\partial_x\phi\partial_x\left(d^\dagger d - \bar{d}^\dagger\bar{d}\right),\\
j_{1,9}^{(3)} &= \mathrm{i}\mu_- v\partial_x\phi\left(d^\dagger\partial_x d - \partial_x d^\dagger d - \bar{d}^\dagger\partial_x\bar{d} + \partial_x\bar{d}^\dagger\bar{d}\right),\\
j_{2,9}^{(2)} &= 2\mu_-\varepsilon\partial_x\theta\left(d^\dagger d - \bar{d}^\dagger\bar{d}\right),\\
j_{4,9}^{(3)} &= \frac{2\mu_-\alpha v}{\sqrt{\pi v}}\partial_x\theta\partial_x\phi\left(d^\dagger d + \bar{d}^\dagger\bar{d}\right)\\
&\quad - \frac{\mathrm{i}\mu_-\alpha v}{\sqrt{\pi v}}\left[d^\dagger d\left(\bar{d}^\dagger\partial_x\bar{d} - \partial_x\bar{d}^\dagger\bar{d}\right) + \left(d\leftrightarrow\bar{d}\right)\right],\\
j_{2,11}^{(3)} &= 2\mathrm{i}\vartheta_-\varepsilon\left[d^\dagger d\left(\bar{d}^\dagger\partial_x\bar{d} - \partial_x\bar{d}^\dagger\bar{d}\right) + \left(d\leftrightarrow\bar{d}\right)\right],\\
j_{2,12}^{(3)} &= 2\kappa_1\varepsilon\partial_x\phi\partial_x\left(d^\dagger d - \bar{d}^\dagger\bar{d}\right),\\
j_{2,13}^{(3)} &= -\,2\kappa_2\varepsilon\partial_x\theta\partial_x\phi\left(d^\dagger d + \bar{d}^\dagger\bar{d}\right),\\
j_{2,14}^{(3)} &= -\,\mathrm{i}\kappa_3\varepsilon\partial_x\phi\left(d^\dagger\partial_x d - \partial_x d^\dagger d - \bar{d}^\dagger\partial_x\bar{d} + \partial_x\bar{d}^\dagger\bar{d}\right).
\end{aligned} \tag{A.6}$$

The calculation of the commutators in equation (A.5) is tedious but straightforward. To simplify the result, we use the known relations for the XXZ model $\varepsilon = 1/m = v$. We find that the conservation law $[J_{\mathrm{E}}, H] = 0$ imposes the constraints

$$\begin{aligned}
g &= -\,\frac{V}{4},\\
g' &= 0,\\
\mu_- &= -\,\frac{\alpha v}{2\sqrt{\pi K}},\\
\mu_+ &= 2\kappa_1,\\
\kappa_2 &= -\,\frac{\alpha^2 v}{2\pi K},\\
\kappa_3 &= 0.
\end{aligned} \tag{A.7}$$

Most importantly, integrability rules out the g' interaction. This is precisely the operator considered in [49] which accounts for a finite decay rate of a mobile impurity in a Luttinger liquid at finite temperatures.

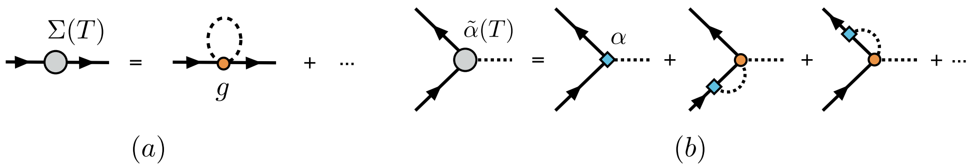

Figure B1. Feynman diagrams at first order in the irrelevant impurity-boson coupling g. (a) Impurity self-energy; (b) vertex correction. The solid line represents the free impurity propagator and the dashed line represents the free boson propagator.

Appendix B. Low temperature corrections to impurity energy and impurity-boson interaction

Here we provide a detailed derivation of equations (12) and (13).

The irrelevant coupling constant g in equation (11) is generated to first order in the interaction term in the *XXZ* model:

$$\mathcal{H}_{\rm int}(j) = \Delta c_j^\dagger c_j c_{j+1}^\dagger c_{j+1}. \tag{B.1}$$

We now use the mode expansion for the fermion field. We bosonize the low-energy fermions in the form $\psi_{\rm R/L}(x) \sim (2\pi\alpha)^{-1/2}{\rm e}^{-{\rm i}\sqrt{2\pi}\varphi_{\rm R/L}(x)}$, where $\varphi_{\rm R/L}(x)$ are chiral boson obeying $[\varphi_{\rm R/L}(x), \partial_{x'}\varphi_{\rm R/L}(x')] = \mp {\rm i}\delta(x - x')$. These are related to the dual bosonic fields by $\varphi_{\rm R/L}(x) = [\theta(x) \mp \phi(x)]/\sqrt{2}$. We focus on the term involving a high energy particle and right movers since the other terms can be obtained by symmetry. The g interaction is generated by taking the combination

$$\begin{aligned}\mathcal{H}_{\rm int}(j) &\sim -{\rm i}\Delta\psi_{\rm R}^\dagger(x)d(x)d^\dagger(x+1)\psi_{\rm R}(x+1) + {\rm h.c.}\\ &= \frac{{\rm i}\Delta}{2\pi}{\rm e}^{{\rm i}\sqrt{2\pi}\varphi_R(x)}{\rm e}^{-{\rm i}\sqrt{2\pi}\varphi_{\rm R}(x+1)}d^\dagger(x)d(x) + {\rm h.c.}\\ &= \frac{\Delta}{2\pi} : \exp\left\{{\rm i}\sqrt{2\pi}\left[\varphi_{\rm R}(x) - \varphi_{\rm R}(x+1)\right]\right\} : d^\dagger(x)d(x) + {\rm h.c.}\\ &\sim -\Delta\left(\partial_x\varphi_{\rm R}\right)^2 d^\dagger(x)d(x),\end{aligned} \tag{B.2}$$

where :: denotes normal ordering with respect to the boson vacuum and we have set the short-distance cutoff to $\alpha = 1$. As a result, we find $g \approx -\Delta$ for $\Delta \ll 1$.

The low-temperature frequency shift is determined by the self-energy $\Sigma(k, \omega, T)$ in

$$G(k, \omega) = \left[\omega - \varepsilon_k - \Sigma(k, \omega, T)\right]^{-1}. \tag{B.3}$$

The self-energy is calculated within perturbation theory in the irrelevant operators. The marginal interaction must be treated nonperturbatively due to the infrared singularities associated with the orthogonality catastrophe. To first order in g the self-energy is independent of k, ω. It is given by the tadpole-type diagram with a single boson propagator illustrated in figure B1 (a). The result is simply

$$\Sigma(T) = 2g\left\langle\left(\partial_x\varphi_{\rm R}\right)^2\right\rangle = \frac{g}{\pi}\left[\frac{\pi/\beta v}{\sin(\pi\epsilon/\beta v)}\right]^2, \tag{B.4}$$

where the factor of 2 accounts for the additional contribution from left movers and ϵ is the point-splitting parameter. Expanding $\left(\sin\frac{\pi\epsilon}{\beta v}\right)^{-2} \approx \left(\frac{\beta v}{\pi\epsilon}\right)^2 + \frac{1}{3}$, we obtain the cutoff-independent term in the impurity self-energy

$$\Sigma(T) = \frac{g\pi T^2}{3v^2}. \tag{B.5}$$

The effective impurity-boson vertex is defined from the three-point function illustrated in figure B1(b). The correction is first order in α and g:

$$\delta\alpha(k, \omega, T) = -4\alpha g\Pi(k, \omega), \tag{B.6}$$

where $\Pi(k, \omega)$ is the Fourier transform of

$$\Pi(x, t) = \langle d(x, t)d^\dagger(0, 0)\rangle\langle\partial_x\varphi_{\rm L}(x, t)\partial_x\varphi_{\rm L}(0, 0)\rangle. \tag{B.7}$$

The vertex correction depends on the external momenta and frequencies. However, to get the correction to the marginal coupling constant α we can set the external momenta to be exactly at the top/bottom of the band (i.e. the state that controls the long-time behavior). For the impurity part of the correlation function we can use the

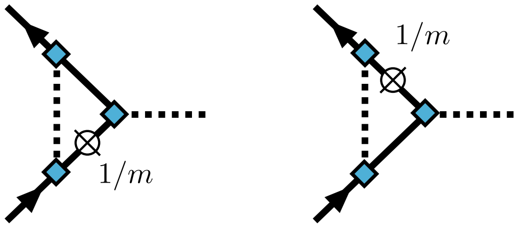

Figure B2. Renormalization of the impurity-boson coupling due to the impurity band curvature in the internal line.

zero temperature propagator

$$\langle Td(x,\,t)d^{\dagger}(0,\,0)\rangle = \theta(t)\mathrm{e}^{-\mathrm{i}\varepsilon t}\delta(x). \tag{B.8}$$

For the free boson propagator, we use the finite temperature expression

$$\langle \partial_x \varphi_{\mathrm{L}}(x,\,t)\partial_x \varphi_{\mathrm{L}}(0,\,0)\rangle = -\frac{1}{2\pi v^2}\frac{(\pi/\beta)^2}{\sinh^2\left[\pi(t+x/v)/\beta\right]}. \tag{B.9}$$

It follows that

$$\begin{aligned}\Pi(k=0,\,\omega=\varepsilon) &= -\frac{\pi}{2\beta^2 v^2}\int_{\epsilon}^{\infty}\mathrm{d}t\,\frac{1}{\sinh^2(\pi t/\beta)}\\ &\approx -\frac{\pi}{2\beta^2 v^2}\left(\frac{\beta^2}{\pi^2\epsilon}-\frac{\beta}{\pi}\right).\end{aligned} \tag{B.10}$$

Dropping the cutoff-dependent term and substituting the temperature-dependent term in equation (B.6), we obtain

$$\delta\alpha(T) = -2\alpha g T/v^2. \tag{B.11}$$

At weak coupling, $\alpha = 2\pi(1-K)\approx 4\Delta$ and $g\approx -\Delta$, thus

$$\delta\alpha/\alpha \approx 2\Delta T. \tag{B.12}$$

However, we only expect the correction to be quantitatively correct when $\delta\alpha/\alpha \approx 2\Delta T \ll 1$.

Going beyond first order in Δ, we find that the leading contributions from dimension-three operators μ_- and μ_+ to Σ and $\delta\alpha/\alpha$ either vanish (in the case of μ_-) or are at least of order Δ^3 (in the case of μ_+; this is because μ_+ is not generated to first order in Δ).

There are, however, corrections at order Δ^2 stemming from the parabolic term in the impurity dispersion

$$\delta\mathcal{H}_m = \frac{1}{2\,m}d^{\dagger}\partial_x^2 d. \tag{B.13}$$

The parabolic dispersion cannot be treated perturbatively in the autocorrelation function for a free impurity, since it is responsible for the $1/\sqrt{t}$ decay of the propagator. However, in the calculation of the renormalized vertex we deal with loop diagrams that contain both impurity and boson propagators integrated over distance x. The impurity Green's function including the dispersion is $G_{\mathrm{imp}}(x,\,t>0) = \mathrm{e}^{-\mathrm{i}\varepsilon t}\sqrt{\frac{\mathrm{i}m}{2\pi t}}\,\mathrm{e}^{\mathrm{i}mx^2/2t}$. The fast oscillation of $G_{\mathrm{imp}}(x,\,t)$ as a function of x implies that integrals like $\int_{-\infty}^{\infty}\mathrm{d}x\;G_{\mathrm{imp}}(x,\,t)F(x,\,t)$, where $F(x,\,t)$ is some correlation function involving the bosonic modes, are dominated by $x\approx 0$. Thus, we can approximate

$$\begin{aligned}\int_{-\infty}^{\infty}\mathrm{d}x\;G_{\mathrm{imp}}(x,\,t)F(x,\,t) &\approx F(0,\,t)\int_{-\infty}^{\infty}\mathrm{d}x\;G_{\mathrm{imp}}(x,\,t)\\ &= \mathrm{e}^{-\mathrm{i}\varepsilon t}F(0,\,t).\end{aligned} \tag{B.14}$$

This is equivalent to using the impurity Green's function in the limit $m\to\infty$, which is simply $G_{\mathrm{imp}}(x,\,t>0)\approx \mathrm{e}^{-\mathrm{i}\varepsilon t}\delta(x)$, as in equation (B.8). On the other hand, expanding the impurity Green's function in powers of $1/m$ yields

$$\begin{aligned}G_{\mathrm{imp}}(x,\,t) &= \mathrm{e}^{-\mathrm{i}\varepsilon t}\int\frac{\mathrm{d}k}{2\pi}\,\mathrm{e}^{\mathrm{i}kx+\mathrm{i}k^2 t/2\,m}\\ &\approx \mathrm{e}^{-\mathrm{i}\varepsilon t}\left[\delta(x)-\frac{\mathrm{i}t}{2\,m}\partial_x^2\delta(x)+\dots\right]\end{aligned} \tag{B.15}$$

The correction involving $\partial_x^2\delta(x)$ within a loop diagram produces an extra power of T. We compute this correction using perturbation theory in $\delta\mathcal{H}_m$. The contribution to the renormalized vertex, shown in figure B2 , is

$$\delta\alpha' = \frac{\alpha^3 v^2}{\pi K m}\int d^2x_1 d^2x_2 d^2x_3\, e^{i\varepsilon t} \times \partial_{x_1}^2 \langle\partial_x\phi(1)\partial_x\phi(0)\rangle\langle d(1)d^\dagger(2)\rangle\langle d(2)d^\dagger(3)\rangle\langle d(3)d^\dagger(0)\rangle. \tag{B.16}$$

The boson propagator is

$$\partial_x^2\langle\partial_x\phi(x)\partial_x\phi(0)\rangle = -\frac{\pi^3 T^4}{2v^4}\frac{2+\cosh[2\pi T(t+x/v)]}{\sinh^4[\pi T(t+x/v)]} + (x\to -x). \tag{B.17}$$

Thus,

$$\begin{aligned}\delta\alpha' &= -\frac{\pi^2\alpha^3 T^4}{Kmv^2}\int_0^\infty dt_1\int_0^{t_1} dt_2\int_0^{t_2} dt_3\,\frac{2+\cosh\left(2\pi T t_1\right)}{\sinh^4(\pi T t)}\\ &= -\frac{\alpha^3 T}{2\pi K m v^2}\left(\frac{3}{\epsilon}-1+\ldots\right).\end{aligned} \tag{B.18}$$

Once again, we keep only the universal T-dependent correction.

Likewise, there is an order $1/m$ correction in the impurity self-energy. The result is given in equation (14) of the main text.

Appendix C. Excitation energies from the thermodynamic Bethe ansatz

In this section we describe the calculation of dressed energies using the thermodynamic Bethe ansatz (TBA) approach to the XXZ model [73, 74].

Bethe ansatz states are parametrized by a set of rapidities $\{x_j^\alpha\}$ which satisfy the Bethe equations. Here j labels the type of string and α specifies a particular rapidity. More precisely, x_j^α refers to the real part of the rapidity, since the imaginary part is fixed by the string hypothesis [73, 74]. Strings with length $n_j > 1$ are interpreted as bound states of n_j particles. For simplicity, we choose the anisotropy parameter to be $\Delta = \cos(\pi/\nu)$, with $\nu \in \mathbb{Z}$. In this case, we can restrict ourselves to a finite number of strings $j = 1, 2,\ldots, \nu$. The strings with $j = 1, 2,\ldots, \nu - 1$ have length $n_j = j$ and parity $\upsilon_j = +1$; the string with $j = \nu$ has length $n_\nu = 1$ and parity $\upsilon_\nu = -1$.

The Bethe equations (in logarithmic form) for a chain of length N and periodic boundary conditions read

$$Nt_j\left(x_\alpha^j\right) = 2\pi I_\alpha^j + \sum_{k=1}^{\nu}\sum_{\beta=1}^{M_k}\Theta_{jk}\left(x_\alpha^j - x_\beta^k\right), \qquad \alpha = 1,\ldots, M_j, \tag{C.1}$$

where M_j is the number of strings of type j in the Bethe ansatz state and I_α^j are integers (for M_j odd) or half-integers (for M_j even). A particular Bethe ansatz wave function is determined by the set of I_α^j's. The functions $t_j(x)$ and the scattering phase shifts $\Theta_{jk}(x)$ are given by

$$t_j(x) = f\left(x;\, n_j,\, v_j\right), \tag{C.2}$$

$$\begin{aligned}\Theta_{jk}(x) &= f\left(x;\, \left|n_j - n_k\right|,\, v_j v_k\right) + f\left(x;\, n_j + n_k,\, v_j v_k\right)\\ &\quad + 2\sum_{l=1}^{\mathrm{Min}\left(n_j,n_k\right)-1} f\left(x;\, \left|n_j - n_k\right| + 2l,\, v_j v_k\right),\end{aligned} \tag{C.3}$$

where we define the function

$$f(x;\, n,\, v) = \begin{cases} 0, & \text{if } n/\nu \in \mathbb{Z},\\ 2\nu\arctan\left\{\left[\cot\left(\dfrac{n\pi}{2\nu}\right)\right]^v \tanh\left(\dfrac{\pi x}{2\nu}\right)\right\}, & \text{otherwise.}\end{cases} \tag{C.4}$$

In the TBA approach, we take the limit $N\to\infty$ and characterize the macroscopic state by the density of particles $\rho(x)$ and density of holes $\rho^h(x)$ in rapidity space. The equilibrium state is obtained by minimizing the free energy as a functional of $\rho(x)$ and $\rho^h(x)$. This leads to a set of coupled nonlinear integral equations for the dressed energies

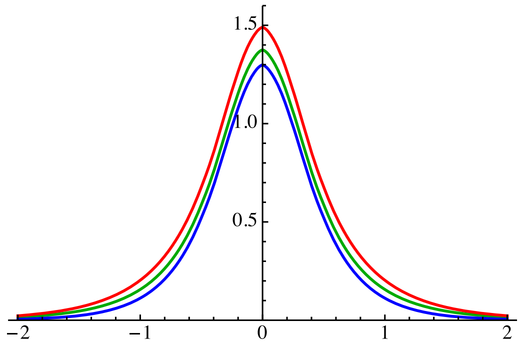

Figure C1. Energy of single one-string excitation as a function of rapidity x for $\Delta = 0.5$ and three different values of temperature. From bottom to top: $T = 10^{-3}$, $T = 0.25$, and $T = 5$.

$$\varepsilon_j(x) = -\,2\nu\,\sin(\pi/\nu)a_j(x) + \frac{1}{\beta}\sum_{k=1}^{\nu} \upsilon_k \int_{-\infty}^{+\infty} \mathrm{d}y\; T_{jk}(x-y)\ln\left[1 + \mathrm{e}^{-\beta\varepsilon_k(y)}\right], \tag{C.5}$$

where $\beta = 1/T$ is the inverse temperature and

$$a_j(x) = \frac{1}{2\pi}\frac{\mathrm{d}t_j}{\mathrm{d}x}, \tag{C.6}$$

$$T_{jk}(x) = \frac{1}{2\pi}\frac{\mathrm{d}\Theta_{jk}}{\mathrm{d}x}. \tag{C.7}$$

Equation (C.5) can be solved numerically by iteration. In the limit $T \to 0$, the dressed energy for $j = 1$ (the even-parity one-string) reduces to the dispersion of the single-hole excitation over the ground state.

The dressed energies can be used to calculate the free energy and other thermodynamic properties [74]. They also show up as the energies of elementary excitations over the equilibrium state [75]. The thermal excitation spectrum for the gapless phase of the *XXZ* model was calculated by Puga [76]. The energy required to create a single hole with rapidity x in the density of type-j strings is

$$\Delta E_j(x) = -\varepsilon_j(x) + \frac{1}{\beta}\sum_{k=1}^{\nu}\frac{\Theta_{kj}(\infty)}{\pi}\ln\left[1 + \mathrm{e}^{-\beta\varepsilon_k(\infty)}\right]. \tag{C.8}$$

Notice that the excitation energies $\Delta E_j(x)$ differ from the dressed energies in equation (C.5) by a constant term that involves all strings.

Figure C1 shows the excitation energy for the $j = 1$ string for three different values of temperature. We are particularly interested in the bandwidth, which is given by $\Delta E_1(0)$. At $T = 0$, the bandwidth is known analytically, $\lim_{T\to 0}\Delta E_1(0) = \frac{\pi\sqrt{1-\Delta^2}}{2\arccos\Delta}$. The important point is that the bandwidth calculated from the TBA dressed energies increases with temperature, contrary to the behavior of the frequencies predicted by the effective field theory and observed numerically using a tDMRG algorithm. This disagreement is rather puzzling given that a generalized TBA approach has even been used to discuss nonequilibrium dynamics [77]. There are two possible explanations: (I) There could be an unexpectedly large time scale required to observe the dynamics governed by low lying TBA excitations, i.e., the TBA frequencies are relevant for the long-time dynamics but we are unable to reach this asymptotic regime numerically. (II) The TBA energies cannot simply be interpreted as those of elementary excitations. While the TBA approach correctly describes the thermodynamics this does not guarantee that such a simple interpretation holds.

Appendix D. Fits of the DMRG data

We have fitted the tDMRG data using the fit function

$$\sqrt{t}\,G(t) = \Gamma + A\left(\frac{\pi T}{\sinh(\pi T t)}\right)^{\tilde{\eta}} \mathrm{e}^{-\mathrm{i}\left(\tilde{\varepsilon}t + \tilde{\varphi}\right)} + B\,t^{-3/2}\mathrm{e}^{-2\mathrm{i}\tilde{\varepsilon}t}\mathrm{e}^{-\rho t} \tag{D.1}$$

where $A,\ B,\ \tilde{\eta},\ \tilde{\varepsilon},\ \tilde{\varphi},\ \rho,\ \Gamma$ are real fitting parameters. The first, constant term Γ is the diffusive contribution. The second term is the single impurity contribution, equation (16) in the main text, while the third term represents the two-impurity contribution, equation (17), where we have allowed for a small decay rate which seems to be of order $\sim\mathrm{e}^{-1/T}$ and might possibly be related to thermal excitations at the band edges. In table D1

Table D1. Parameters obtained by fitting the tDMRG data presented in the main text, see figures 1 and 2

	Δ	T	Fit range	Γ	A	$\tilde{\eta}$	$\tilde{\varepsilon}$	$\tilde{\varphi}$	B	ρ
theory	0.3	0	—	0	—	0.838	1.1835	0.530	—	—
th. $\mathcal{O}(\Delta)$	0.3	0.07	—	2.11×10^{-5}	—	0.831	1.1825	0.520	—	—
fit	0.3	0.07	$t \geqslant 10$	$\sim$0	0.275	0.796	1.185	0.751	−0.202	0
th. $\mathcal{O}(\Delta)$	0.3	0.25	—	7.94×10^{-4}	—	0.814	1.1709	0.493	—	—
fit	0.3	0.25	$t \geqslant 10$	6.3×10^{-4}	0.421	0.713	1.165	1.990	−0.242	0.016
theory	0.8	0	—	0	—	0.629	1.465	0.202	—	—
th. $\mathcal{O}(\Delta)$	0.8	0.167	—	5.58×10^{-4}	—	0.533	1.457	0.052	—	—
fit	0.8	0.167	$t \geqslant 15$	3.26×10^{-4}	0.161	0.403	1.503	−0.238	0	—
th. $\mathcal{O}(\Delta)$	0.8	0.25	—	1.26×10^{-3}	—	0.492	1.448	−0.013	—	—
fit	0.8	0.25	$t \geqslant 15$	9.88×10^{-4}	0.210	0.387	1.525	−0.397	0	—

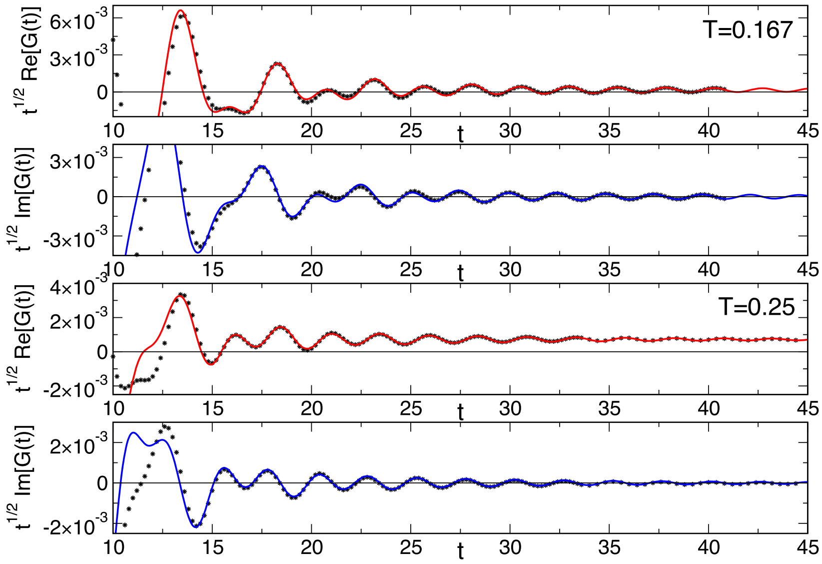

Figure D1. $\sqrt{t}\,G(t)$ at $\Delta = 0.5$: tDMRG data (symbols) and fits (lines) for $t \geqslant 15$. The fit parameters are given in table D2.

Table D2. Parameters for various fits of the tDMRG data at $\Delta = 0.5$.

	Δ	T	Fit range	Γ	A	$\tilde{\eta}$	$\tilde{\varepsilon}$	$\tilde{\varphi}$	B	ρ
theory	0.5	0	—	0	—	3/4	1.30	0.393	—	—
th. $\mathcal{O}(\Delta)$	0.5	0.167	—	3.98×10^{-4}	—	0.710	1.2919	0.329	—	—
fit 1	0.5	0.167	$t \geqslant 10$	1.68×10^{-4}	0.277	0.575	1.294	0.853	−0.086	0.019
fit 2	0.5	0.167	$t \geqslant 15$	1.49×10^{-4}	0.199	0.527	1.287	1.406	−0.099	0.020
fit 3	0.5	0.167	$t \geqslant 20$	1.51×10^{-4}	0.284	0.558	1.285	1.853	−0.093	0.019
th. $\mathcal{O}(\Delta)$	0.5	0.25	—	1.09×10^{-3}	—	0.690	1.2829	0.299	—	—
fit	0.5	0.25	$t \geqslant 15$	$7.19 \cdot 10^{-4}$	0.266	0.501	1.272	2.196	−0.091	0.041

we present the fit parameters for the fits shown in figures 2 and 3. We also present the theoretical predictions for Γ, equation (24), and for other parameters based on weak-coupling expressions (to first order in Δ) for the coupling constants of irrelevant operators (rows labeled 'th. $\mathcal{O}(\Delta)$').

One of our main findings based on the analysis of the numerical data is that the two-impurity contribution becomes very small for large interaction strengths leading to a fit parameter B for $\Delta = 0.8$ which is essentially zero. To further support that B for the considered temperatures is strongly reduced with interaction, we present in figure D1 below tDMRG data and fits for intermediate interaction strength $\Delta = 0.5$.

Here a two-impurity contribution is still visible but the amplitude B is already very small, see table D2 . In order to illustrate the sensitivity of the fit parameters on the fit interval we concentrate on the case $\Delta = 0.5$, $T = 0.167$ and show in table D2 parameters for fits using three different time intervals.

Except for the phase shift $\tilde{\varphi}$, and, to a lesser extent, the amplitude $\tilde{A}$, all fit parameters show little variation implying, in particular, that it is possible to extract the temperature dependence of $\tilde{\varepsilon}(T)$ and $\tilde{\eta}(T)$ with reasonably accuracy from the tDMRG data. On the other hand, we want to emphasize that the phase shift $\tilde{\varphi}$ cannot be fixed reliably from numerical data even at zero temperature, see [22, 23].

References

[1] Sachdev S 1999 *Quantum Phase Transitions* (Cambridge: Cambridge University Press)
[2] Fukuhara T *et al* 2013 *Nat. Phys.* **9** 235
[3] Knap M, Kantian A, Giamarchi T, Bloch I, Lukin M D and Demler E 2013 *Phys. Rev. Lett.* **111** 147205
[4] Langen T, Geiger R, Kuhnert M, Rauer B and Schmiedmayer J 2013 *Nat. Phys.* **9** 640
[5] Hild S *et al* 2014 *Phys. Rev. Lett.* **113** 147205
[6] Bisogni V *et al* 2014 *Phys. Rev. Lett.* **112** 147401
[7] Kinoshita T *et al* 2006 *Nature* **440** 900
[8] Rigol M, Dunjko V, Yurovsky V and Olshanii M 2007 *Phys. Rev. Lett.* **98** 050405
[9] Cazalilla M A 2006 *Phys. Rev. Lett.* **97** 156403
[10] Gangardt D M and Pustilnik M 2008 *Phys. Rev.* A **77** 041604(R)
[11] Calabrese P, Essler F H L and Fagotti M 2011 *Phys. Rev. Lett.* **106** 227203
[12] Rozhkov A 2005 *Eur. Phys. J.* B **47** 193
[13] Carmelo J M P, Penc K and Bozi D 2005 *Nucl. Phys.* B **725** 421
Carmelo J M P, Penc K and Bozi D 2006 *Nucl. Phys.* B **737** 351
[14] Pustilnik M, Khodas M, Kamenev A and Glazman L I 2006 *Phys. Rev. Lett.* **96** 196405
[15] Pereira R G, Sirker J, Caux J-S, Hagemans R, Maillet J M, White S R and Affleck I 2006 *Phys. Rev. Lett.* **96** 257202
Pereira R G, Sirker J, Caux J-S, Hagemans R, Maillet J M, White S R and Affleck I 2007 *J. Stat. Mech.* P08022
[16] Khodas M, Pustilnik M, Kamenev A and Glazman L I 2007 *Phys. Rev.* B **76** 155402
[17] Imambekov A and Glazman L I 2009 *Science* **323** 228
[18] Matveev K A and Andreev A V 2011 *Phys. Rev. Lett.* **107** 056402
[19] Matveev K A and Furusaki A 2013 *Phys. Rev. Lett.* **111** 256401
[20] Pustilnik M and Matveev K A 2014 *Phys. Rev.* B **89** 100504(R)
[21] Imambekov A, Schmidt T L and Glazman L I 2012 *Rev. Mod. Phys.* **84** 1253
[22] Pereira R G, White S R and Affleck I 2008 *Phys. Rev. Lett.* **100** 027206
[23] Pereira R G, White S R and Affleck I 2009 *Phys. Rev.* B **79** 165113
[24] Kitanine N, Kozlowski K K, Maillet J M, Slavnov N A and Terras V 2012 *J. Stat. Mech.* P09001
[25] Shashi A, Panfil M, Caux J-S and Imambekov A 2012 *Phys. Rev.* B **85** 155136
[26] Sirker J and Klümper A 2005 *Phys. Rev.* B **71** 241101(R)
[27] Barthel T, Schollwöck U and White S R 2009 *Phys. Rev.* B **79** 245101
[28] Karrasch C, Bardarson J and Moore J 2012 *Phys. Rev. Lett.* **108** 227206
[29] Karrasch C, Bardarson J and Moore J 2013 *New J. Phys.* **15** 083031
[30] Barthel T, Schollwöck U and Sachdev S arXiv:1212.3570
[31] Vidal G 2004 *Phys. Rev. Lett.* **93** 040502
[32] White S R and Feiguin A E 2004 *Phys. Rev. Lett.* **93** 076401
[33] Daley A, Kollath C, Schollwöck U and Vidal G 2004 *J. Stat. Mech.* P04005
[34] Schmitteckert P 2004 *Phys. Rev.* B **70** 121302(R)
[35] Bañuls M C, Hastings M B, Verstraete F and Cirac J I 2009 *Phys. Rev. Lett.* **102** 240603
[36] White S R 1992 *Phys. Rev. Lett.* **69** 2863
[37] Schollwöck U 2011 *Ann. Phys.* **326** 96
[38] Panfil M and Caux J-S 2014 *Phys. Rev.* A **89** 033605
[39] Korepin V E, Bogoliubov N M and Izergin A G 1993 *Quantum Inverse Scattering Method and Correlation Functions* (Cambridge: Cambridge University Press)
[40] Sirker J, Pereira R G and Affleck I 2009 *Phys. Rev. Lett.* **103** 216602
Sirker J, Pereira R G and Affleck I 2011 *Phys. Rev.* B **83** 035115
[41] Lukyanov S 1998 *Nucl. Phys.* B **522** 533
[42] Thurber K R, Hunt A W, Imai T and Chou F C 2001 *Phys. Rev. Lett.* **87** 247202
[43] Xiao F *et al* 2015 *Phys. Rev.* B **91** 144417
[44] Karrasch C, Hauschild J, Langer S and Heidrich-Meisner F 2013 *Phys. Rev.* B **87** 245128
[45] Grossjohann S and Brenig W 2010 *Phys. Rev.* B **81** 012404
[46] Duan L-M, Demler E and Lukin M D 2003 *Phys. Rev. Lett.* **91** 090402
[47] Giamarchi T 2004 *Quantum Physics in One Dimension* (Oxford: Clarendon)
[48] Sirker J 2006 *Phys. Rev.* B **73** 224424
[49] Castro Neto A H and Fisher M P A 1996 *Phys. Rev.* B **53** 9713
[50] Karzig T, Glazman L I and von Oppen F 2010 *Phys. Rev. Lett.* **105** 226407
[51] Klümper A and Sakai K 2002 *J. Phys. A: Math. Gen* **35** 2173
[52] Lukyanov S and Terras V 2003 *Nucl. Phys.* B **654** 323
[53] Bloembergen N 1949 *Physica* **15** 386
[54] de Gennes P G 1958 *J. Phys. Chem. Solids* **4** 223
[55] Steiner M, Villain J and Windsor C G 1976 *Adv. Phys.* **25** 87
[56] Carboni F and Richards P M 1968 *J. Appl. Phys.* **39** 967
[57] Böhm M, Leschke H, Henneke M, Viswanath V S, Stolze J and Müller G 1994 *Phys. Rev.* B **49** 417
[58] Böhm M, Viswanath V S, Stolze J and Müller G 1994 *Phys. Rev.* B **49** 15669
[59] Fabricius K, Löw U and Stolze J 1997 *Phys. Rev.* B **55** 5833
[60] Fabricius K and McCoy B M 1998 *Phys. Rev.* B **57** 8340

[61] Starykh O A, Sandvik A W and Singh R R P 1997 *Phys. Rev.* B **55** 14953
[62] Boucher J P, Bakheit M A, Nechtschein M, Villa M, Bonera G and Borsa F 1976 *Phys. Rev.* B **13** 4098
[63] Takigawa M, Motoyama N, Eisaki H and Uchida S 1996 *Phys. Rev. Lett.* **76** 4612
[64] Kikuchi J, Kurata N, Motoya K, Yamauchi T and Ueda Y 2001 *J. Phys. Soc. Japan.* **70** 2765
[65] Takigawa M, Asano T, Ajiro Y, Mekata M and Uemura Y J 1996 *Phys. Rev. Lett.* **76** 2173
[66] Pratt F L, Blundell S J, Lancaster T, Baines C and Takagi S 2006 *Phys. Rev. Lett.* **96** 247203
[67] Prosen T 2011 *Phys. Rev. Lett.* **106** 217206
[68] Pereira R G, Pasquier V, Sirker J and Affleck I 2014 *J. Stat. Mech.* P09037
[69] Prosen T 2014 *Nucl. Phys.* B **886** 1177
[70] Castella H, Zotos X and Prelovšek P 1995 *Phys. Rev. Lett.* **74** 972
[71] Zotos X, Naef F and Prelovsek P 1997 *Phys. Rev.* B **55** 11029
[72] Hofferberth S, Lesanovsky I, Fischer B, Schumm T and Schmiedmayer J 2007 *Nature* **449** 324
[73] Takahashi M and Suzuki M 1972 *Prog. Theor. Phys.* **48** 2187
[74] Takahashi M 1999 *Thermodynamics of One-Dimensional Solvable Models* (Cambridge: Cambridge University Press)
[75] Korepin V E, Bogoliubov N M and Izergin A G *Quantum Inverse Scattering Method and Correlation Functions* (Cambridge: Cambridge University Press)
[76] Puga M W 1980 *J. Math. Phys.* **21** 2307
[77] Caux J-S and Essler F H L 2013 *Phys. Rev. Lett.* **110** 257203